1 Pattern Component Modeling

Our final analysis was a implementation of a pattern component modelling (PCM) approach to factorial multivariate analysis, using the cross-validated mahalanobis distance [1]. Briefly, we tested whether the dissimilarity matrix of observed activity patterns could be decomposed into a linear combination of contrast matrices generated from our factorial design. Each hypothesis matrix (contrasts matrices corresponding to our factors, such as main effects and interaction) was tested for its ability to explain unique variance in the dissimilarity matrix (or here, the estimated second-moment matrix) using an ordinary least squares regression. While we have described how PCM is formally equivalent to the CVMANOVA approach, it has unique advantages in terms of the simplicity of its implementation.

1.1 Representational Similarity Analysis (RSA)

RSA is an method for quantifying the pairwise similarity of patterns of voxel activity between experimental conditions [2]. Unlike multi-voxel classification [3], which test the performance of machine-learning classifiers categorize conditions on the basis of multi-voxel activity patterns, contemporary RSA allows for the ratio-scale measurement of pattern similarity, producing more reliable estimates of condition-specific patterns of activity [4]. Here, we implemented the cross-validated squared Mehalanobis distance (or, Linear Discriminant Contrast; LDC) as our measure of pattern similarity, as it allows for an unbiased estimate of the true distance between patterns, i.e., the expected value is zero when the true patterns are identical [1]. Previous work has found this distance measure to be more reliable and noise-tolerant than other measures of pattern similarity, such as correlation distance and non-cross-validated squared Mehalanobis distances [4]. It should be noted that while the analysis we implemented is technically the cross-validated Euclidean distance, these measures are equivalent when there is no spatial covariance, as was the case in our simulation. The LDC between conditions i and j over M runs is defined as,

$$\hat{d}^2_{i,j} = \sum_{l,m;l\neq m}^{M} \left(\hat{u}_i^{(m)} - \hat{u}_j^{(m)}\right)^T \left(\hat{u}_i^{(l)} - \hat{u}_j^{(l)}\right) / M(M-1))$$

Where u hat is a vector of voxel activity estimates for each condition (typically beta weights from a first-level general linear model), taken from runs m and l. From this matrix of dissimilarity matrix, we can generate the second-moment matrix (or, G matrix), which includes an estimate of the variance of each condition's activity pattern. This is necessary for estimating condition-unique patterns for the interaction factor. The G matrix can be derived from the LDC matrix by centring with respect to the mean pattern across conditions. Using the LDC matrix D, for k conditions,

$$\hat{G} = -\frac{1}{2} HDH^T$$

where

$$H = I_k - 1_k / k$$

The G matrix can also calculated independently from the LDC, as the variance-covariance matrix of activity patterns over conditions, a complementary (if not simpler) approach to to the one taken in this experiment.

1.2 Pattern Component Modelling (PCM)

PCM tests whether an observed dissimilarity matrix can be decomposed into a hypothesized set of independent components. In this case, we used multiple linear regression to estimate the weight matrix that that minimized the squared difference between our simulated G matrix and a set of factorial contrasts. This analysis assumes that our components are orthogonal, an assumption that is reasonable for random vectors (i.e., activity patterns) in high-dimensional space. For c contrasts H1 ... Hc, we estimate the weight matrix b_c that minimizes the difference between our basis matrices G_c and our observed G matrix,

$$G = \sum_c G_c b_c$$

where

$$G_c = H_c (H_c^T H_c)^{-1} H_c^T$$

and

$$X = \left[vec(G_1), vec(G_2), ..., vec(G_c) \right]$$
$$\hat{b} = (X^T X)^{-1} X^T vec(\hat{G})$$

where the vec operator strings these matrices out into a vector. For this experiment, our contrasts correspond to the full factorial design: two main effects and and their interaction (see Figure 1). While the interaction contrast is not independent of the main effects (as addressed in the previous methods), the calculation of these matrices's pseudoinverse orthogonalized these contrasts in order to estimate the unique contribution of each contrast for the prediction of the dissimilarity matrix.

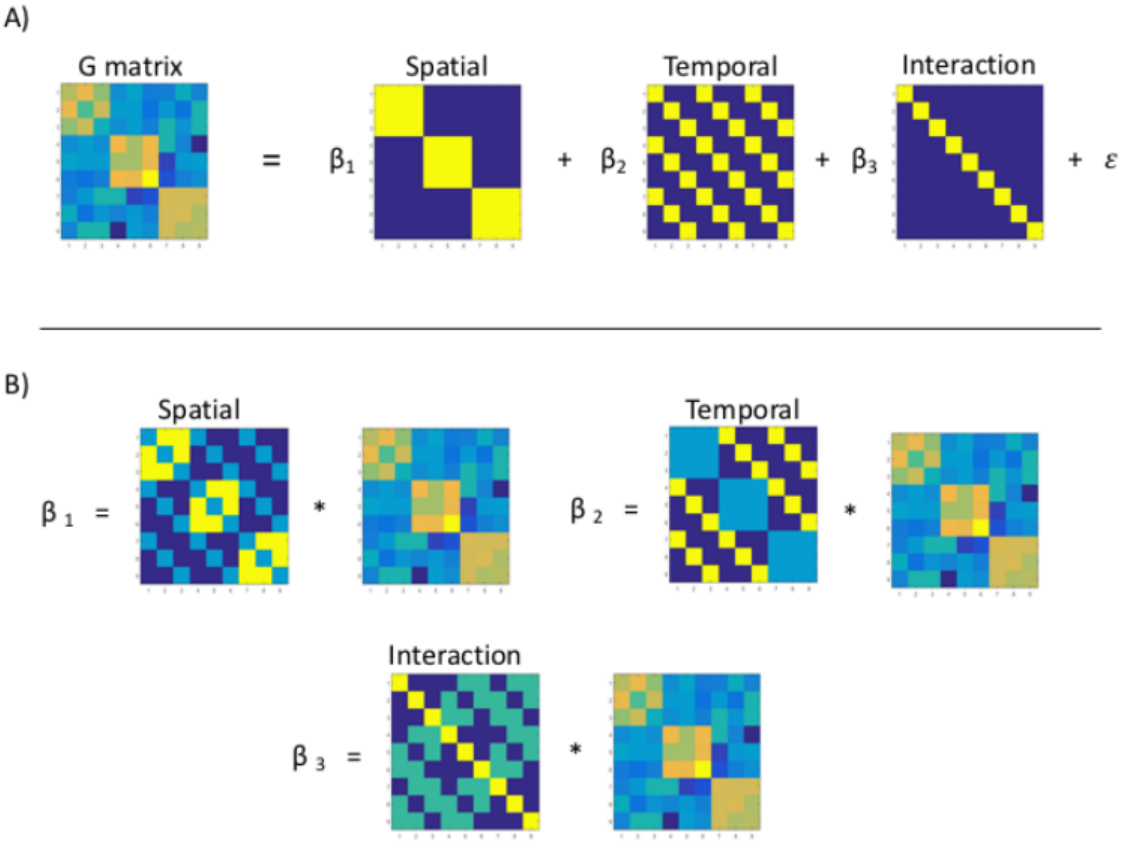

Figure 1: Schematic of the pattern component model used in this experiment. A) The cross-validated G matrix is shown comprising of a linear combination of the basis matrices corresponding to the three contrasts of our factorial design, plus some error. B) The regression weights in A are shown to be generated using an OLS estimation: multiplying the pseudoinverse of the set contrast matrices by our estimated G matrix (here, shown separately). We can see that the peudoinverse of our basis matrices are orthogonal. The basis matrix of the intercept is not shown.

2 Results

We generated 10 000 simulations of datasets containing combinations of factors (i.e., main effects or interactions) with signal strengths of [0 .05 .1 .15] SNR. For each combination of factors, we generated a null distribution by permuting the order of the conditions within each run. This provides a less stringent hypothesis test than a model with all factors but the factor-of-interest included. However, by examining the false positive rate

for the factor-of-interest in all of our models where it is not present, we can still estimate the contribution of other factors on (incorrectly) detecting our factor-ofinteract. We took the 95th percentile of these permuted distributions as our critical boundary, calculated the proportion of simulations that had larger regression weights. While our unbiased measure of pattern similarity can produce negative weights due to noise, signals will always produce a positive weight, requiring this one-tailed test of significance. In Figure 2 we show the rate of H0 rejection for a main effect (A) and interaction (B) regression weight for combinations of factors with .15 SNR. We can see that the presence of other factors does not not alter the H0 rejection rejection rate when the factor is present or absent, allowing us to confidently use the permuted null distributions. We can see that there is good sensitivity and selectivity for main effects and interactions at all combinations of factor effects. In Figure 2 we can see that as the SNR increases, there are dramatic increases in the sensitivity of our test.

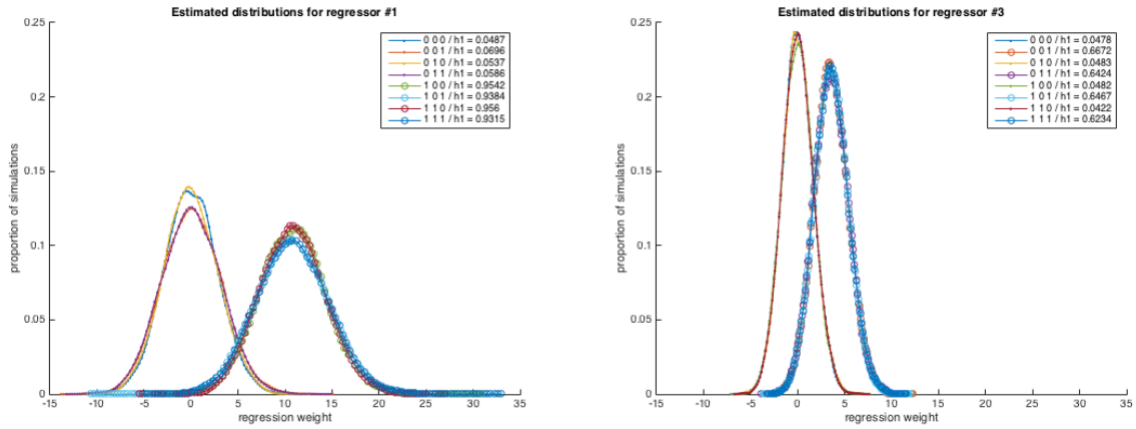

Figure 2: The distributions of regression weights for combinations of factors at .15 SNR for regressor one (Main Effect) and regressor three (Interaction). Distributions with unbroken lines are signal-absent trials, and lines with circles are signal-present trials. There is good sensitivity and specificity with this approach, regardless of the other factors present in the simulation, although there is a slight increase in type 1 error when only interaction effects are present. Legend: (Left) The combination of 0s and 1s correspond to the absence and presence of factors, respectively [main effect 1, main effect 2, interaction]. (Right) h1 values corresponds to the proportion of simulations with regression weights greater than the 95th percentile of the permuted distribution for that combination of conditions.

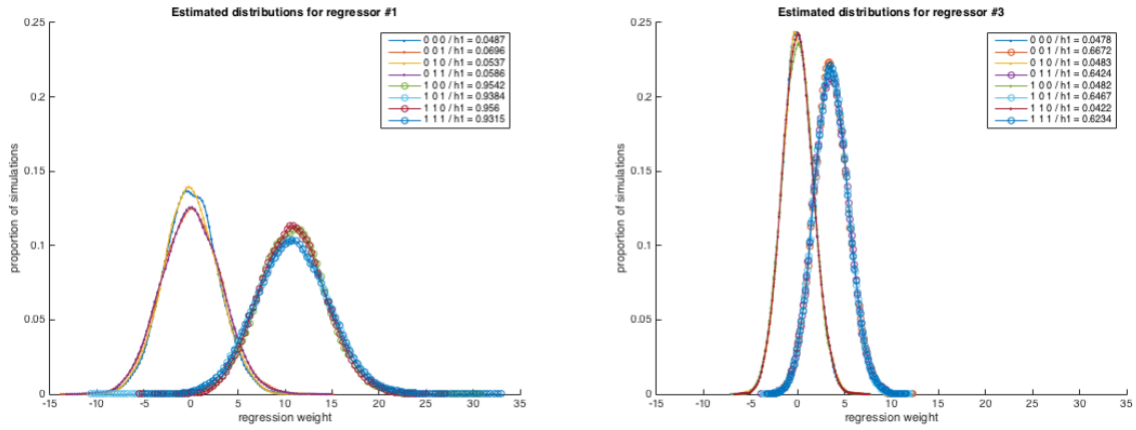

Figure 3: Figure 3. The power of our test at different SNRs for Regressor 1 (main effect) and regressor 3 (interaction). The critical value corresponds to the 95th percentile of the permuted distribution of the strongest SNR. As the SNR increases, there is a dramatic increase in power. Legend: (Left) The SNR of the factor-of-interest. (Right) The power at that SNR.

References

[1] Alexander Walther, Naveed Ejaz, Nikolaus Kriegeskorte, Jörn Diedrichsen, and Jörn Diedrichsen. Representational fmri analysis: an introductory tutorial.

[2] Nikolaus Kriegeskorte, Marieke Mur, and Peter A Bandettini. Representational similarity analysis-connecting the branches of systems neuroscience. *Frontiers in systems neuroscience*, 2:4, 2008.

[3] James V Haxby, M Ida Gobbini, Maura L Furey, Alumit Ishai, Jennifer L Schouten, and Pietro Pietrini. Distributed and overlapping representations of faces and objects in ventral temporal cortex. *Science*, 293(5539):2425–2430, 2001.

[4] Alexander Walther, Hamed Nili, Naveed Ejaz, Arjen Alink, Nikolaus Kriegeskorte, and Jörn Diedrichsen. Reliability of dissimilarity measures for multi-voxel pattern analysis. *NeuroImage*, 2015.